Theoretical Calculations on Silica Frameworks and Their Correlation with Experiment

Neil J. Henson,[†] Anthony K. Cheetham,[*,†] and Julian D. Gale[‡]

Materials Department, University of California, Santa Barbara, California 93106, and Chemistry Department, Imperial College of Science and Technology, South Kensington, London SW7 2AZ, UK

Received February 1, 1994. Revised Manuscript Received June 21, 1994[⊗]

Symmetry-constrained lattice energy minimizations have been performed on a series of pure silica polymorphs using the shell model for silicates. Quantitative agreement is found between the experimental and calculated structures with particularly good agreement being obtained for the fractional coordinates of the atoms in the asymmetric unit. The computed lattice energies of the silicas are found to be between 8 and 20 kJ mol^{-1} less than that of quartz. The energies are found to be directly dependent on the densities of the structures and show good agreement with a recent calorimetric study.

Introduction

The recent calorimetric measurements of Petrovic and co-workers[1] have provided intriguing insights into the relationship between the crystal structure of open silicate frameworks and their stability. In particular, they reported that the open-framework silica structures are between 7 and 14 kJ mol^{-1} less stable than quartz. The observed trends in the data were ascribed to differences in the distributions of Si–O–Si bond angles rather than, for instance, any direct dependence on the density. These results provide an interesting challenge in the computational area, since it is now possible to treat silica frameworks routinely by using the techniques of lattice energy minimization using interatomic potentials.[2] Several empirical force fields have been developed[3–5] which can accurately reproduce relative energies and structural properties such as cell parameters, bond lengths, and bond angles. These are based on electrostatic two-body terms, summed either with an Ewald summation or the use of a tapering function, combined with Buckingham-type nonbonded two-body terms or explicit Morse functions. In addition, a three-body term is often included to correctly represent the O–T–O bond angle, and a well-established shell model potential has been derived in an attempt to represent the polarizability of the O atom in the lattice.[5]

In this work we describe constant pressure lattice energy minimizations using the shell model for silicates developed by Sanders[5] and imposing the full crystallographic symmetry of the experimental structures as an additional constraint. The theoretical results are compared directly with the thermochemical measurements of Petrovic et al. and with fractional atomic coordinates obtained in recent crystallographic studies of siliceous zeolites.

Methods and Models

Details of Force Field. The force field for silicates derived by Sanders[5] is based on a formal charge model and fitted to the crystal structure and elastic and dielectric constants of α-quartz. The formal charge model has the advantage that it is compatible with a wide variety of potentials derived for other ionic solids and allows defects to be easily included in the system with no uncertainties in the charge state.

The interaction between ions i and j is represented by a Buckingham potential plus a Coulombic term to describe the electrostatics:

$$E_{ij} = A_{ij}\exp\left(\frac{r_{ij}}{\varrho_{ij}}\right) - \frac{C_{ij}}{r_{ij}^{6}} + \frac{q_i q_j}{r_{ij}}$$

The electrostatic energy is calculated by an Ewald summation[6] with the relevant cutoffs for the individual summations in real and reciprocal space chosen to minimize the total number of terms.[7] This is weighted by a factor which relates the relative computational expense of the real and reciprocal terms. The cutoff is chosen to give accuracy to eight significant figures in the lattice energy. The short-range Buckingham potential is evaluated to a cutoff of 12 Å. The residual dispersion energy due to atoms lying beyond this distance is corrected by the continuum approximation.

The oxygen ions are modeled using the shell model of Dick and Overhauser.[8] All short-range forces act on a massless oxygen shell which is coupled to the oxygen core, from which it is coulombically screened, through a harmonic function:

$$E_{\text{core-shell}} = {}^1/_2 k_{ij}(r_{\text{core}} - r_{\text{shell}})^2$$

This allows the effective polarizability of each oxygen ion to vary as a function of its environment in the system. Three-body forces are also included in the force field for the O–Si–O

* To whom correspondence should be addressed.
† Materials Department, UCSB.
‡ Imperial College.
⊗ Abstract published in *Advance ACS Abstracts,* August 15, 1994.
(1) Petrovic, I.; Navrotsky, A.; Davis, M. E.; Zones, S. I. *Chem. Mater.* **1993**, *5*, 1805.
(2) Jackson, R. A.; Catlow, C. R. A. *Mol. Simulation* **1988**, *1*, 207. Kramer, G. J., Farragher, N. P.; van Beest, B. W. H.; van Santen, R. A. *Phys. Rev.* **1991**, *B43*, 5008. de Man, A. J. M.; Jacobs, P. J. H.; Gilson, J. P.; van Santen, R. A.; *Zeolites* **1992**, *12*, 826.
(3) de Vos Burchart, E.; Verheij, V. A.; van Bekkum, H.; van de Graaf, B. *Zeolites* **1992**, *12*, 183.
(4) Kramer, G. J.; de Man, A. J. M.; van Santen, R. A. *J. Am. Chem. Soc.* **1991**, *113*, 6435.
(5) Sanders, M. J.; Leslie, M.; Catlow, C. R. A. *J. Chem. Soc., Chem. Commun.* **1984**, 1271.
(6) Ewald, P. P. *Ann. Phys.* **1921**, *64*, 253.
(7) Catlow, C. R. A.; Norgett, M. J. *AERE Harwell Rep.* **1976**, M2936.
(8) Dick, B. G.; Overhauser, A. W. *Phys. Rev.* **1958**, *112*, 90.

0897-4756/94/2806-1647$04.50/0

Table 1. Comparison of Calculated and Experimental Cell Parameters for Silicas

	a(Å)	b(Å)	c(Å)	α (deg)	β (deg)	γ (deg)
α-quartz (experiment)	4.913	4.913	5.406	90.0	90.0	120.0
α-quartz (calculation)	4.835	4.835	5.346	90.0	90.0	120.0
α-cristobalite (expt)	4.978	4.978	6.948	90.0	90.0	90.0
α-cristobalite (calc)	4.970	4.970	7.000	90.0	90.0	90.0
β-cristobalite (expt)	5.063	5.063	7.160	90.0	90.0	90.0
β-cristobalite (calc)	4.995	4.995	7.177	90.0	90.0	90.0
low-*T* tridymite (expt)	18.494	4.991	23.758	90.0	105.8	90.0
low-*T* tridymite (calc)	18.540	4.983	23.824	90.0	105.8	90.0
high-*T* tridymite (expt)	18.494	4.991	25.832	90.0	117.8	90.0
high-*T* tridymite (calc)	18.533	4.981	25.901	90.0	117.8	90.0
ZSM-12 (exp)	24.863	5.012	24.328	90.0	107.7	90.0
ZSM-12 (calc)	24.954	4.998	24.151	90.0	107.4	90.0
silicalite (expt)	20.060	13.360	19.800	90.0	90.0	90.0
silicalite (calc)	20.073	13.335	19.693	90.0	90.0	90.0
monoclinic silicalite (expt)	19.879	20.107	23.826	90.0	145.9	90.0
monoclinic silicalite (calc)	19.740	19.979	23.656	90.0	145.7	90.0
ZSM-11 (expt)	20.067	20.067	13.411	90.0	90.0	90.0
ZSM-11 (calc)	19.995	19.995	13.452	90.0	90.0	90.0
SSZ-24 (expt)	13.603	13.603	8.277	90.0	90.0	120.0
SSZ-24 (calc)	13.679	13.679	8.466	90.0	90.0	120.0
FAU (expt)	24.258	24.258	24.258	90.0	90.0	90.0
FAU (calc)	24.226	24.226	24.226	90.0	90.0	90.0

bond angle in the form of a harmonic angle bending potential:

$$E_{ijk} = {}^1/_2 k_{ijk}(\theta - \theta_0)^2$$

where θ_0 is the equilibrium tetrahedral bond angle.

The program GULP (general utility lattice program) developed by Gale[9] was used for all the calculations.

Models for Silicates. We considered a series of silica polymorphs for which thermochemical measurements have previously been made, and also a wide range of other zeolite structures and "dense" silica polymorphs. Also we examined a number of hypothetical siliceous structures which are analogues to well-characterized aluminophosphates, $AlPO_4$-n.

We have used the following structural data for the silicas in question. For silicalite, we have considered both the orthorhombic structure of Flanigen et al.[10] and the low-temperature monoclinic phase[11] (since our calculations are correspond to 0 K). For ZSM-11 and ZSM-12, we used the structural determinations of Fyfe and co-workers.[12,13] In the case of tridymite, we took both the low- and high-temperature forms for the minimizations.[14,15] For cristobalite, we again considered the low-temperature tetragonal[16] and high-temperature cubic structures[17] and in addition the tetragonal $I\bar{4}2d$ structure proposed by Wright and Leadbetter for β-cristobalite.[18] For the faujasite structures, we examined the cubic siliceous structure recently reported by Hriljac et al.[19] and also the hexagonal EMT structure of Newsam et al.[20] The SSZ-24 structure was that of Bialek and co-workers.[21] The structures of ferrierite and dodecasil were taken from recent powder and single-crystal studies of those materials.[22,23] All the structures were treated as purely siliceous. We also considered the recently characterized structure of moganite[24] and the structure of stishovite,[25] a high-density silica polymorph containing octahedral silicon. The structural references for the other silicates considered in this study are given in refs 26–37.

Results

There are a number of questions to be considered when comparing computational results to those of experiments in this area. For example, since our work represents energies calculated at 0 K, it would be useful to perform free energy minimizations to assess the effect if any of thermal expansion on the relative energies of the structures. Nevertheless, the comparisons reveal some interesting features.

Structure and Properties. In all cases the lattice parameters are reproduced to within 2% of the experimental values. Table 1 shows the comparison for several structures. In relation to the fractional coordinates of the individual atoms, we wish to stress that the agreement with experiment is particularly good for

(9) GULP (the General Utility Lattice Program) written and developed by J. D. Gale, Royal Institution/Imperial College, UK, 1992–4.

(10) Flanigen, E. M.; Bennett, J. M.; Grose, R. W.; Cohen, J. P.; Patton, R. L.; Kirchner, R. M.; Smith, J. V. *Nature* **1978**, *271*, 512.

(11) van Koningveld, H.; Jansen, J. C.; van Bekkum, H. *Zeolites* **1990**, *10*, 235.

(12) Fyfe, C. A.; Gies, H.; Kokotailo, G. T.; Pasztor, C.; Strobl, H.; Cox, D. E. *J. Am. Chem. Soc.* **1989**, *111*, 2470.

(13) Fyfe, C. A.; Gies, H.; Kokotailo, G. T.; Marler, B.; Cox, D. E. *J. Phys. Chem.* **1990**, *94*, 3718.

(14) Kato, K.; Nukui, A. *Acta. Crystallogr.* **1976**, *B32*, 2486.

(15) Baur, W. H. *Acta. Crystallogr.* **1977**, *B33*, 2615.

(16) Dollase, W. A. *Z. Kristallogr. Bd.* **1965**, *121*, 369.

(17) Wyckoff, R. W. G. *Crystal Structures*; Interscience: New York, 1965.

(18) Wright, A. F.; Leadbetter, A. J. *Philos. Mag.* **1975**, *31*, 1391.

(19) Hriljac, J. A.; Eddy, M. M.; Cheetham, A. K.; Donahue, J. A.; Ray, G. J. *J. Solid State. Chem.* **1993**, *106*, 66.

(20) Newsam, J. M.; Treacy, M. M. J.; Vaughan, D. E. W.; Strohmaier, K. G.; Mortier, W. J. *J. Chem. Soc., Chem. Commun.* **1989**, 493–495.

(21) Bialek, R.; Meier, W. M.; Davis, M. E.; Annen, M. J. *Zeolites* **1991**, *11*, 438.

(22) Morris, R. E.; Weigel, S. J.; Henson, N. J.; Bull. L. M.; Cheetham, A. K., submitted for publication.

(23) Weigel, S. J.; Guttierez Puebla, E.; Monge Bravo, A.; Henson, N. J.; Bull, L. M.; Cheetham, A. K., to be published.

(24) Miehe, G.; Graetsch, H. *Eur. J. Mineral.* **1992**, *4*, 693.

(25) Baur, W. H.; Khan, A. A. *Acta. Crystallogr.* **1971**, *B27*, 2133.

(26) Richardson, J. W.; Vogt, E. T. C. *Zeolites* **1992**, *12*, 13.

(27) Gramlich-Meier, R.; Gramlich, V.; Meier, W. M. *Am. Mineral.* **1985**, *80*, 619.

(28) Bennett, J. M.; Richardson, J. M.; Pluth, J. J., Smith, J. V. *Zeolites* **1987**, *7*, 160.

(29) Bennett, J. M.; Kirchner, R. M. *Zeolites* **1992**, *12*, 338.

(30) Simmen, A.; McCusker, L. B.; Baerlocher, Ch.; Meier, W. M. *Zeolites* **1991**, *11*, 654.

(31) Gramlich, V., Meier, W. M. *Z. Kristallogr., Kristallgeom., Kristallphys., Kristallchem.* **1971**, *133*, 134.

(32) Alberti, A.; Davoli, P.; Vezzalini, G.; *Z. Kristallogr.* **1986**, *175*, 249.

(33) Behrens, P.; van de Goor, G.; Wiebcke, M.; Braunbarth, C.; Schneider, A. M.; Felsche, J.; Engelhardt, G.; Fischer, P.; Fuetterer, K.; Depmeier, W., submitted to the *Proceedings of the 8th International Symposium on Molecular Recognition and Inclusion*, Ottawa, 1994.

(34) Calligaris, M.; Nardin, G.; Randaccio, L.; Comin Chiaramonti, P. *Acta Crystallogr.* **1982**, *B38*, 602.

(35) Newsam, J. M.; Treacy, M. M.; Koetsier, W. T.; DeGruyter, C. B. *Proc. R. Soc. London* **1988**, *A420*, 375.

(36) Rudolph, P. R.; Crowder, C. E. *Zeolites* **1990**, *10*, 163.

(37) Lobo, R. F., personal communication.

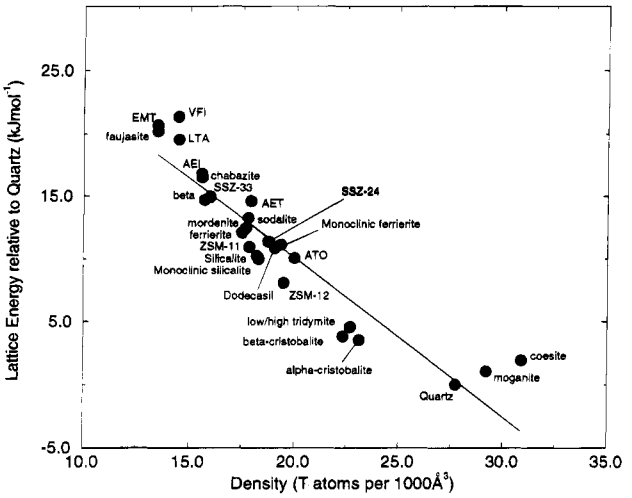

Figure 1. Variation of calculated lattice energy with density for silica structures.

Table 2. Comparison of Calculated and Experimental Structural Parameters for Siliceous Faujasite

cell parameter (Å)			
expt	24.2576(3)		
calc	24.226		
fractional coordinates (esd's in parentheses)			
	x	*y*	*z*
Si(1)			
exp	0.94608(8)	0.12530(8)	0.03589(9)
calc	0.94597	0.12571	0.03590
O(1)			
exp	0.0000	0.89377(6)	0.10623(6)
calc	0.0000	0.89309	0.10691
O(2)			
expt	0.99677(6)	0.99677(6)	0.14066(9)
calc	0.99773	0.99773	0.14057
O(3)			
exp	0.07570(6)	0.07570(6)	0.96423(9)
calc	0.07604	0.07604	0.96423
O(4)			
expt	0.07063(7)	0.07063(7)	0.32115(10)
calc	0.07027	0.07027	0.32146

those siliceous structures that have been well-determined by diffraction measurements, for example, the cubic faujasite structure (see Table 2). This finding suggests that some of our computed structures may be more accurate than the corresponding experimental ones, especially those based upon poor-quality X-ray powder data.

As has been shown previously,[3,4] the calculated lattice energies of the structures show a direct correlation with the density (Figure 1). Kramer and co-workers[4] employed an unphysically large dispersion term which gives an anomalously large range in energy for the silicas considered; this required an additional correction term to be added to give the correct experimental range. The dispersive term in the Sanders potential is more consistent with theoretical estimations of the O–O interaction.[38] We have also used a larger short-range cutoff (12 Å) than Kramer et al. and estimated the contribution of interactions beyond this distance with the continuum approximation.

In the case of the tridymite, both low- and high-temperature structures essentially give the same minimized lattice energy. This may stem from the combination of the uncertainties in the calculated energies and the small range that is spanned by the complete family of the structures. The proposed tetragonal structure for β-cristobalite is found to be 6 kJ mol^{-1} lower in energy than the cubic *Fd3m* structure, in agreement with a previous quantum mechanical study of this structure,[39] and we also find that the low-temperature monoclinc phase of silicalite is slightly more stable (~0.5 kJ mol^{-1}) than the room-temperature orthorhombic polymorph. The cell parameters of the monoclinic structure are reproduced to within 1% of experiment.

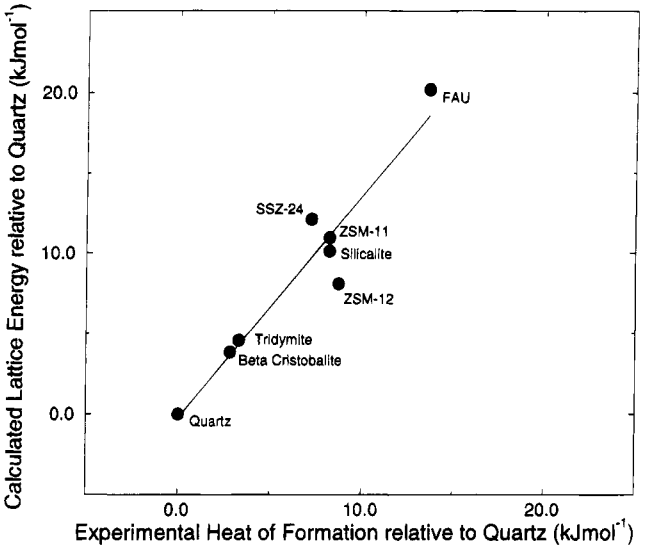

Figure 2. Correlation of the experimental heat of formation with the calculated lattice energy relative to quartz. (i) The EMT structure is omitted because the structure contains a large amount of aluminum and therefore cannot be considered as siliceous. (ii) The lattice energy is related to the heat of formation by a Born–Haber cycle and, to a very good approximation, the two quantities differ by a constant term. (iii) Experimental data for quartz are taken from ref 40, for cristobalite from ref 41, for tridymite from ref 42, and the remaining values from ref 1.

In an attempt to rationalize the density dependence of the lattice energy, we factorized the total energy into the contributions from the Coulombic, short-range attractive and repulsive, and the three-body terms. Of these terms, the only one that shows a systematic increase with density is the attractive short-range interaction, but the variation is nonlinear and is therefore insufficient to account for the observed trend. However, we should note that the fitting method that was used to develop the force field introduces considerable uncertainty into the breakdown of the various contributions to the total energy.

A most encouraging aspect of the calculations is that they show very good quantitative agreement with the experiment calorimetric data (Figure 2), with the open-framework structures predicted to be 8–20 kJ mol^{-1} less stable than quartz. Furthermore, when data on the nonzeolitic silicas are included, the experimental ener-

(38) Fowler, P. W. *Mol. Phys.* **1985**, *56*, 83.

(39) Liu, F.; Garofalini, S. H.; King-Smith, R. D.; Vanderbilt, D. *Phys. Rev. Lett.* **1993**, *70*, 2750.

(40) CODATA Task Group, CODATA recommended key values for thermodynamics, 1975; *J. Chem. Thermodyn.* **1976**, *8*, 603.

(41) Richet, P.; Bottinga, Y.; Denielou, L.; Petitet, J. P.; Tequi, C. *Geochim. Cosmochim. Acta* **1982**, *46*, 2639.

(42) Robie, R. A.; Hemingway, B. S.; Fisher, J. R. *Geol. Survey. Bull.* **1979**, 1452.

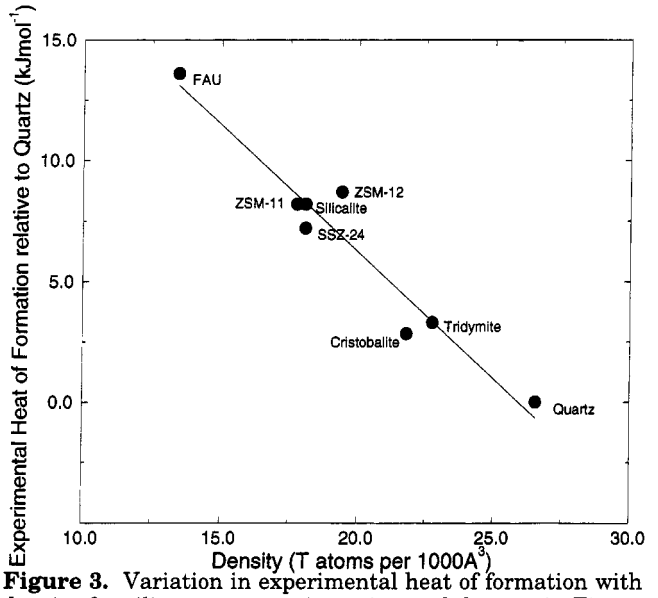

Figure 3. Variation in experimental heat of formation with density for silica structures (experimental data as in Figure 2).

gies do indeed correlate well with density (Figure 3). In particular, for those structures having densities lower than that of quartz, there is a direct dependence of lattice energy on density. However, moganite, coesite, and stishovite, all of which are denser than α-quartz, are predicted to be of higher energy. This result correlates with experiment[1] showing quartz to be the energy minimum in the series but suggests that the dependence of lattice energy on density does not hold for all silica structures. In the case of stishovite, we predict a lattice energy that is about 100 kJ mol^{-1} greater than for quartz, which is a large overestimate of the experimental value. The deficiencies in the prediction of the lattice energy and structure of stishovite are probably due to an inability of the force field to correctly represent six-coordinated silicon. It would be useful to include structures beyond the lower end of the density range of those presented here, the recently synthesised mesoporous silica in the MCM-41 family being good candidates. However it must be stressed that these structures are not pure silica materials and currently available thermochemical data for these system cannot be considered in the present context.

Phonon Spectra. The calculated phonon modes for several of the silica structures at the Γ point show imaginary frequencies suggesting that the experimental space group used in the minimizations is incorrect. In an attempt to elucidate how the structures are inclined to break their assumed symmetry, we performed additional calculations relaxing the symmetry of the structures to the space group $P1$ and allowing the imaginary phonon modes to further optimize the structures. For example, the orthorhombic phase of silicalite minimizes to a final structure with a large number of negative phonon frequencies. This structure is found to relax to the monoclinic phase with space group $P2_1/c$ if the symmetry constraints are removed, which is the correct low-temperature structure. In addition, we also find that the structure of ferrierite has a tendency to reduce its symmetry from primitive orthorhombic to C-centered monoclinic (from $Pmnn$ to $C2/m$).

We conclude that the computational treatments of these silica systems are now sufficiently robust that they bear quantitative comparison with both structural and thermochemical properties and can be used explore the relative stabilities and structures of framework silicas for which there is no reliable experimental data.

Acknowledgment. The authors would like to thank the Science and Engineering Research Council, Los Alamos National Laboratory, and Biosym Technologies for financial support throughout this work. This work was also supported by the UCSB-MRL under National Science Foundation Award No. DMR-9123048. We also acknowledge Dr. Antonio Redondo and Prof. Ray Dupree for useful discussions.